Received: 13 June 2019 | Revised: 28 July 2019 | Accepted: 18 October 2019

DOI: 10.1002/lio2.322

ORIGINAL RESEARCH

Laryngoscope Investigative Otolaryngology

Effects of thyroplasty implant stiffness on glottal shape and voice acoustics

Brian H. Cameron BA[1] | Zhaoyan Zhang PhD[2] | Dinesh K. Chhetri MD[2]

[1]Keck School of Medicine of USC, Los Angeles, California

[2]UCLA Department Head and Neck Surgery, Los Angeles, California

Correspondence
Dinesh K. Chhetri, MD, UCLA Department Head and Neck Surgery, Los Angeles, CA.
Email: dchhetri@mednet.ucla.edu

Funding information
National Institutes of Health, Grant/Award Numbers: R01 DC011300, R01 DC009229

Abstract

Objectives: Vocal fold (VF) stiffness and geometry are determinant variables in voice production. Type 1 medialization thyroplasty (MT), the primary surgical treatment for glottic insufficiency, changes both of these variables. Understanding the cause and effect relationship between these variables and acoustic output might improve voice outcomes after MT. In this study, the effects of thyroplasty implants with variable stiffness on glottal shape and acoustics were investigated.

Methods: In an ex vivo human larynx phonation model, bilateral MT with implants of four stiffness levels (1386, 21.6, 9.3, and 5.5 kPa) were performed. Resulting acoustics and aerodynamics were measured across multiple airflow levels. A vertical partial hemilaryngectomy was performed and stereoscopic images of the VF medial surface taken to reconstruct its three-dimensional (3D) surface contour. The results were compared across implants.

Results: The effects of implant stiffness on acoustics varied by airflow. Softer implants resulted in improved acoustics, as measured by cepstral peak prominence (CPP), at lower airflow levels compared to stiffer implants but this relationship reversed at high airflow levels. Stiffer implants generally required less airflow to generate a given subglottal pressure. Stiffer implants resulted in greater medialized surface area and maximal medialization, but all implants had similar effects on overall VF medial surface contour.

Conclusion: Softer implants result in less medialization but better acoustics at low airflow rates. Stiffer implants provide better acoustics and more stable pressure-flow relationships at higher airflow rates. This highlights a potential role for patient-specific customized thyroplasty implants of various stiffness levels.

Level of Evidence: NA.

KEYWORDS

acoustics, glottal shape, thyroplasty, voice production, voice quality

This study is an oral presentation at the 140th Annual Meeting of the American Laryngological Association, Austin, TX, 5/1-5/3.

A Special Visual Abstract has been developed for this paper

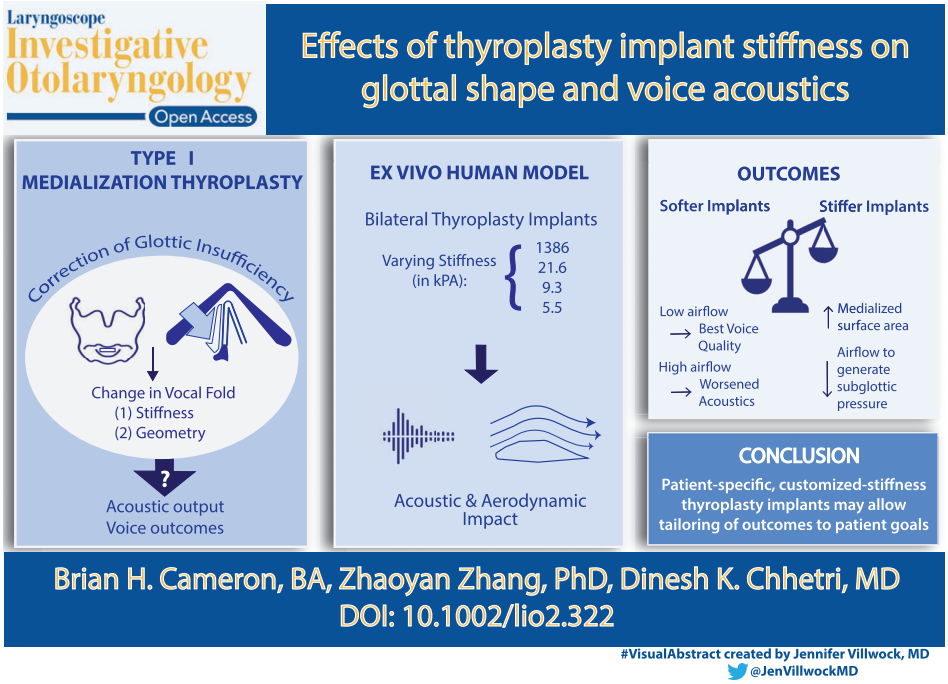

1 | INTRODUCTION

Voice production is a combination of complex biomechanical processes involving neuromuscular events that change vocal fold physiological properties and aerodynamic events that initiate and maintain glottal vibration. The changes in physiological properties are controlled by the intrinsic laryngeal muscles, and include changes in glottal channel shape (width, length, height, and contour) and vocal fold stiffness. These properties in turn, directly affect the interaction of the vocal folds with the glottal airflow and thus are the primary determinants of the produced voice type.[1-3] Neuromuscular abnormalities affecting laryngeal muscles such as paresis, paralysis, or atrophy lead to glottic insufficiency, one of the most common causes of dysphonia. The goal of treatment is to improve glottal channel shape and stiffness through muscle strengthening or by physically medializing the impaired vocal fold with implants in the paraglottic space. Treatment modalities for glottic insufficiency include voice therapy, injection laryngoplasty, and medialization thyroplasty (MT).[4-6]

Currently, the main goal in the treatment of glottic insufficiency is to improve voice by improving glottic closure. The target outcome is measured by direct visualization of the glottic closure from a superior endoscopic view of the larynx. However, theoretical, computational, physical modeling, and ex vivo studies all have attributed a significant role for glottal contour and vocal fold stiffness in controlling acoustic and aerodynamic parameters such as cepstral peak prominence (CPP), harmonics-to-noise ratio (HNR), fundamental frequency (F_0), and phonation threshold pressure.[7-13] During medialization thyroplasty, both glottal contour and vocal fold body stiffness are altered concurrently by the implant shape and stiffness. However, the roles of implant stiffness and medial surface shape in optimizing phonation remain unclear and unexplored.[7] The difficulty in visualizing the medial surface shape and measuring tissue stiffness in vivo has contributed to a poor understanding of these parameters and their effects.

Hirano's cover-body model presented a model for voice production that separated the vocal fold biomechanically into body and cover layers that interact to control phonation type.[14-16] Augmentation of the vocal fold with procedures like MT changes the vocal fold contour and stiffness and impacts this body-cover interaction. The objectives of this study are to analyze the effects of thyroplasty implants of varying stiffnesses on glottal channel shape and acoustics. We chose to study soft implants because previous studies suggested that softer implants, which more accurately reflect the stiffness of native tissue, may result in improved acoustics.[7] Still, the mechanism by which softer implants affect acoustics remains unclear. We hypothesize that the medial surface shape and body stiffness have effects on the resulting acoustics and aerodynamics of voice.

2 | METHODS AND MATERIALS

2.1 | Ex vivo larynx phonation

Permission was obtained from University of California, Los Angeles, Department of Pathology and Laboratory Medicine to obtain human tissue for research from the autopsy suite. Adult human larynges were obtained within the first 48 hours postmortem and were immediately

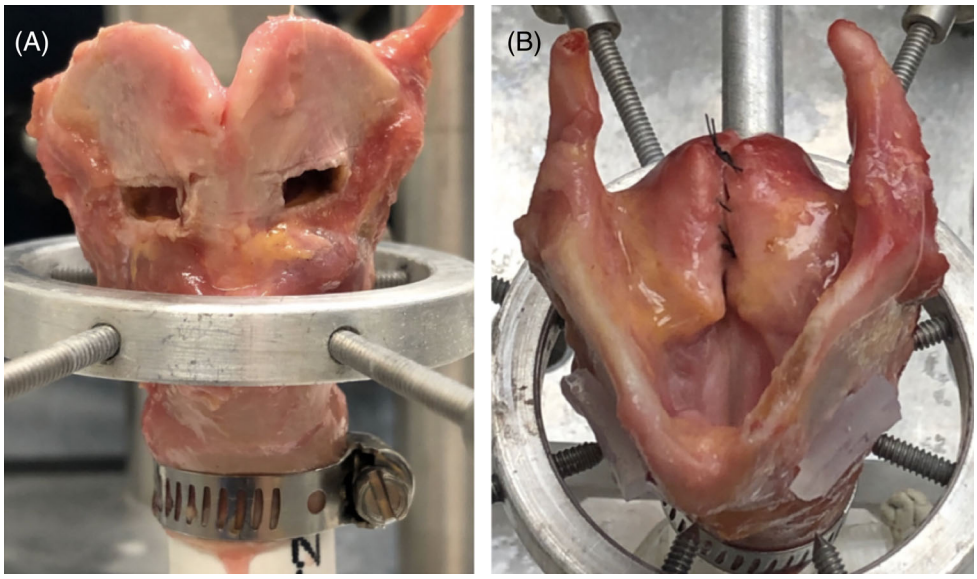

FIGURE 1 A, Anterior view of experimental larynx set-up showing thyroplasty windows without implants. B, Superior camera view of larynx with bilateral implants in place. Implants were carved so vocal folds just touched each other at glottal midline

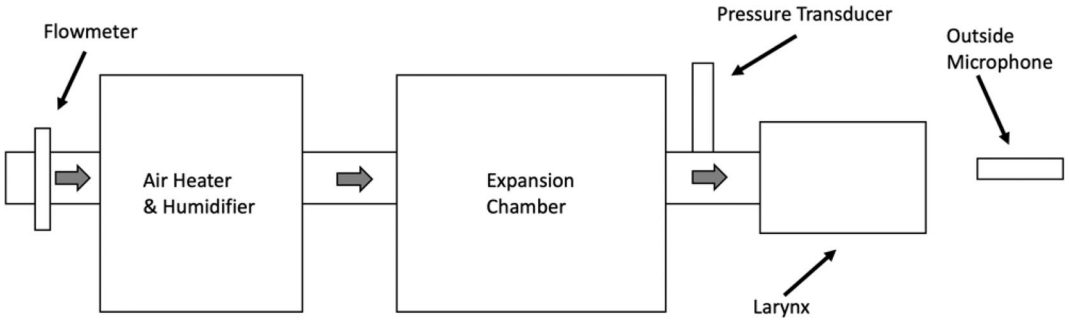

FIGURE 2 Diagram of the experimental setup

Implant #	I1	I2	I3	I4
Material	Silastic	Silicone	Silicone	Silicone
Ratio of components: A:B:thinner	N/A	1:1:1	1:1:2	1:1:3
Implant Young's modulus (kPa)	1386	21.6	9.3	5.5

TABLE 1 Implants and larynges used in current study

Notes: Implant 1 was purchased as a pre-made block used for MT. Implants 2 to 4 were made by combining silicone polymers (A, B), with a thinner solution. L1 = Larynx 1, 62-year-old male; L2 = Larynx 2, 83-year-old female; L3 = Larynx 3, 67-year-old female.

stored in a freezer at −80°C. The day before the experiment, each larynx was stored overnight at −4°C, and the day of each experiment it was soaked in phosphate buffered saline solution until completely thawed. The supraglottic structures of the larynx were removed to visualize the vocal folds with a high-speed camera situated superiorly. The posterior commissure was closed with sutures between the arytenoids to reduce the need for excessive airflow rates to initiate phonation and minimize potential effects of posterior opening on phonation. Type 1 thyroplasty was performed as described by Isshiki with minor modifications.[5] Rectangular thyroplasty windows were created bilaterally using an otologic drill. The inferior edge of the window was parallel to and 2 mm from the inferior border of the thyroid cartilage and the superior edge was just below the level of the vocal folds. The height of the window was about 4 to 5 mm and length about 9 mm (Figure 1).

An excised larynx phonation set-up was used as previously described.[12] A total of three larynges were used for this study (L1—Male, age 62; L2—Female, age 83; L3—Female, age 67). The larynges were attached at tracheal rings 2 to 3 to a 1.5 cm interior diameter polyvinyl chloride (PVC) pipe using an O-ring, forming an air-tight seal (Figures 1 and 2). Compressed air was then sent through an upstream flowmeter, heated to 37°C, humidified to 100%, and discharged into an expansion chamber that mimicked a lung reservoir (inner dimensions $42 \times 42 \times 48$ cm). Air then flowed through the attached pipe and larynx to initiate phonation (Figures 1 and 2). A pressure transducer was attached to the pipe to measure subglottal pressure. An

external microphone, 25 cm away from the larynx, recorded the radiated outside acoustic pressure.

2.2 | Preparation of silicone implants

Four implants with Young's moduli of 1386, 21.6, 9.3, and 5.5 kPa were used. The first implant (1386 kPa, I1) was carved from a silicone block (802-M Medical Grade Silicone Block, Technical Products of GA, Georgia) currently used for MT at UCLA. Its stiffness was previously measured using an instrumented indentation system.[16] The softer implants were made by combining the two components of a silicone liquid polymer (Ecoflex 0030; Smooth On Inc, Easton, Pennsylvania) with a silicone thinner solution at different ratios to achieve varying degrees of stiffness as previously published.[7] The two silicone components and the thinner solution were combined at a ratio of 1:1:1 (21.6 kPa, I2), 1:1:2 (9.3 kPa, I3), and 1:1:3 (5.5 kPa, I4) (Table 1). These stiffnesses were selected based on prior physiologic stiffness measurements of human and canine VF tissue (2-8 kPa) as well as the stiffnesses used previously in studies using physical models.[11,16,17] I1 was first hand carved from the silastic block by the senior laryngologist to a custom size that achieved enough medialization for the vocal fold to just touch each other at the glottal midline (Figure 1B). Then, using I1 as a template, I2 to I4 were carved as exact replicas with <0.05 mm of difference between implants. All implants achieved complete glottal closure when viewed from superior direction in each larynx.

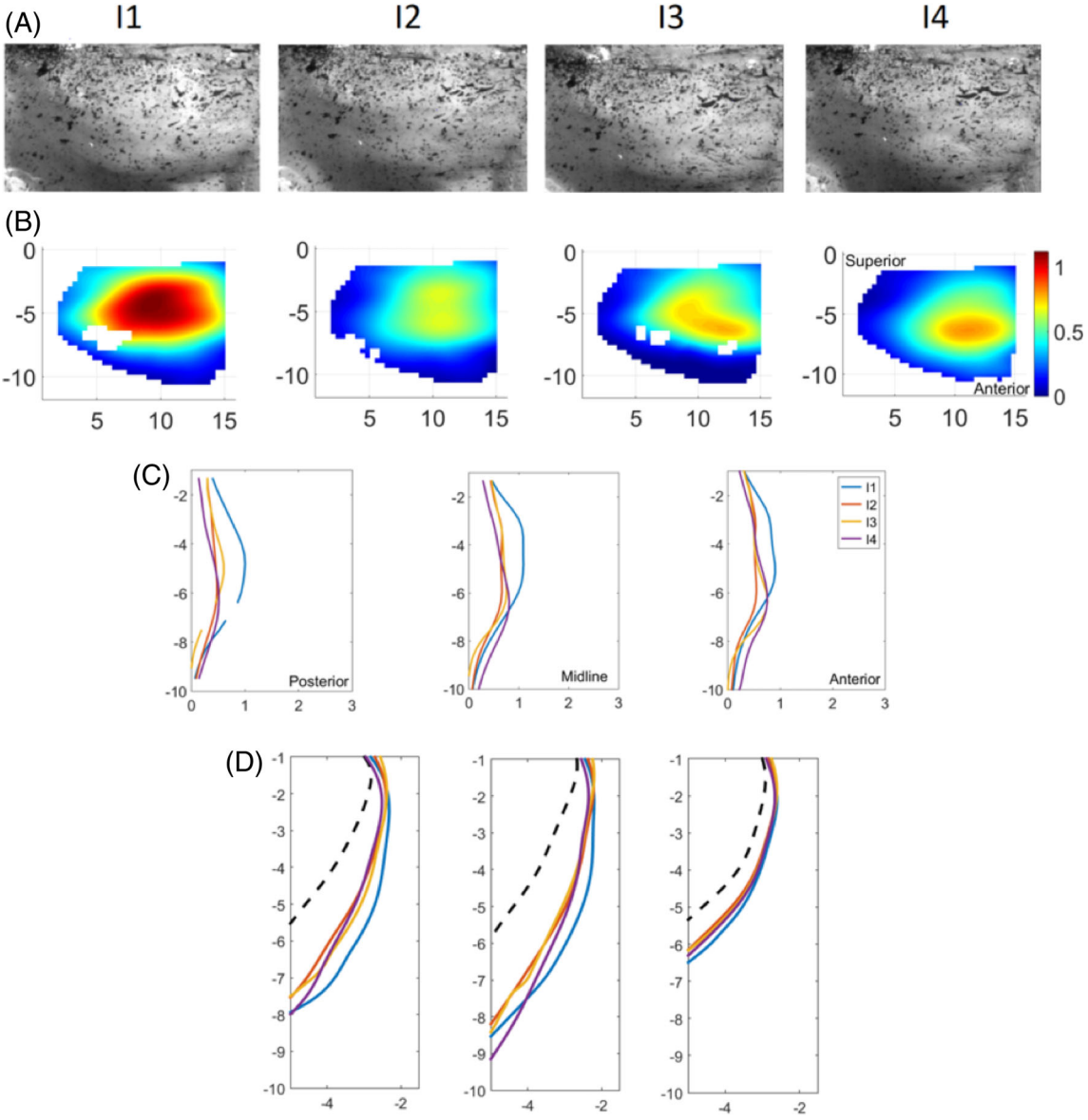

FIGURE 3 Images of medial surface of L2 (83F) for each implant. A, vocal fold medial surface imaged through one prism base for each implant. Black specks represent graphite powder markings used for 3D imaging analysis. B, Medial surface displacement measured for each implant. Images are for corresponding photographic images above. C, Coronal sections of the medial surface displacement for each implant (implant 1 = blue, 2 = orange, 3 = yellow, 4 = purple) at three anterior–posterior sections. D, Coronal sections of medial surface contour. Black dashed line = baseline. All dimensions listed in above images are in millimeters

2.3 | Measurement of subglottal pressure and acoustic signals

For each larynx, a previously described[12,18] flow-ramp phonation procedure was used for each implant. Each implant was inserted carefully, as to not damage tissue. Use of humidified air during phonation and regular misting of the larynx with saline prevented tissue fatigue. Airflow was slowly increased while mean flow rate, mean subglottal pressure, and outside acoustic pressure were recorded at multiple points throughout. For analysis, we noted the onset of phonation, and measured the acoustics/aerodynamics at designated flow rates of 200, 400, and 600 mL/s. Acoustic and aerodynamic signals were analyzed using MATLAB (MATLAB release 2015a, the Mathworks, Inc, Natick, Massachusetts). Mean CPP, mean HNR and mean F_0 were calculated using VoiceSauce software plugin.[19] Both CPP and HNR are currently most reliable measures of acoustic quality with higher values indicating better acoustic quality.

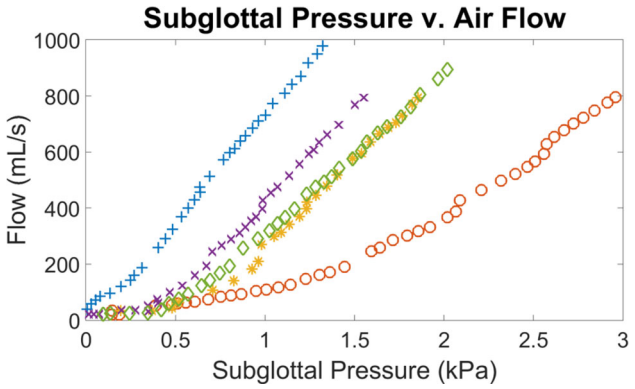

FIGURE 4 Subglottal pressure vs airflow relationship by Implant type during ex vivo larynx phonation for L2. In general, higher subglottal pressure was reached at lower airflow levels with stiffer implants. + = baseline, O = Implant 1, * = Implant 2, x = Implant 3, ◊ = Implant 4

2.4 | Preparation of hemilarynx

Subsequent to ex vivo phonation, vertical hemilaryngectomy was performed to expose one hemilarynx for vocal fold medial surface contour mapping. The medial surface was then sprayed with face foundation (Y3, Era Beauty, erabeauty.com) and lightly dusted with graphite powder (General Pencil Company, Inc, Jersey City, New Jersey) to increase the surface contrast for 3D imaging calculations from recorded images (Figure 3A).

2.5 | Calculation of surface displacement and interpretation of data

The hypotenuse of a right-angle glass prism was placed along the anatomic midline of the glottis from the anterior commissure to posterior commissure of the hemilarynx. This prism displayed two distinct stereoscopic views of the VF medial surface, which were imaged with a

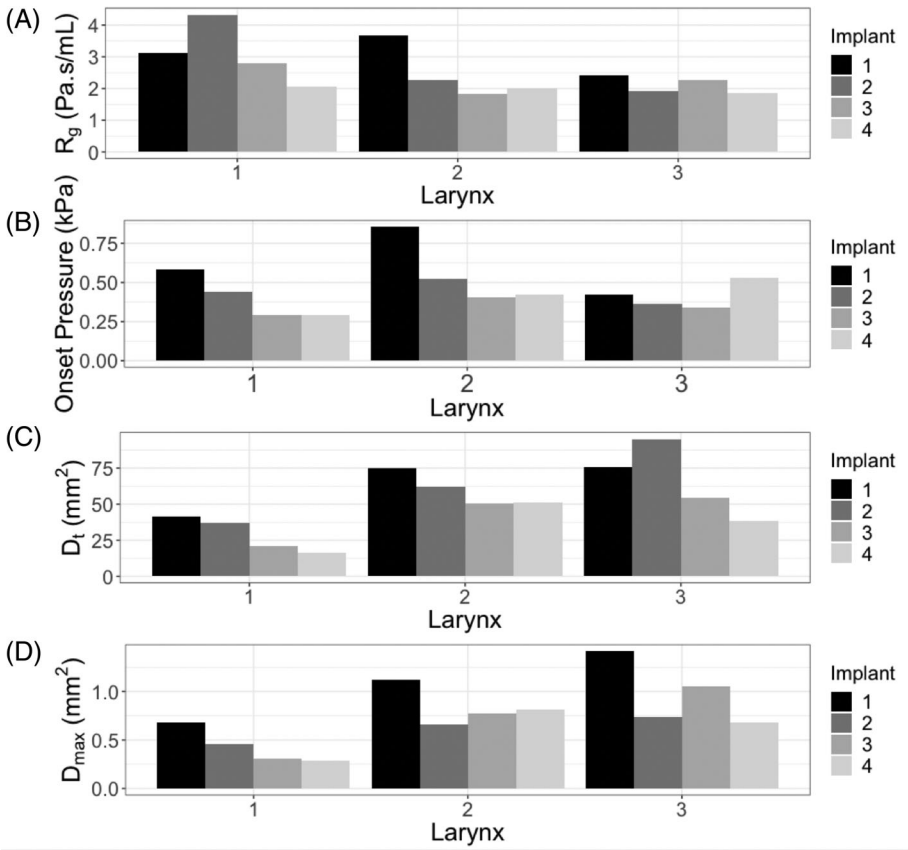

FIGURE 5 A, Glottal resistance (R_g); B, onset pressure; C, total displaced medial surface area (D_t); *D*, maximum medial surface displacement (D_{max}) averaged across all airflow rates for each implant. (Implant 1 = 1386 kPa, 2 = 21.6 kPa, 3 = 9.3 kPa, 4 = 5.5 kPa)

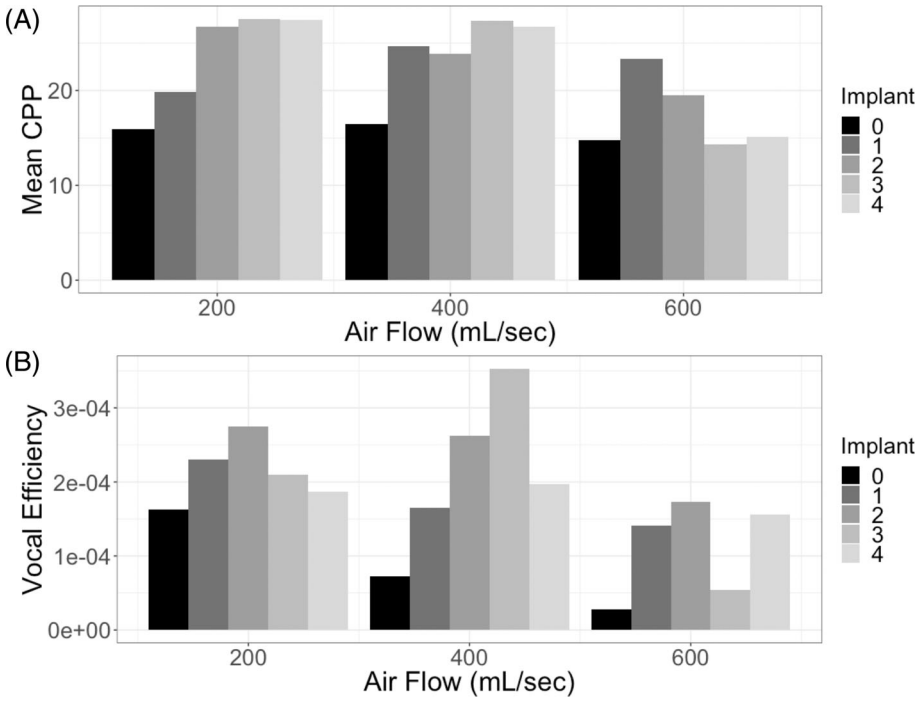

FIGURE 6 A, Mean cepstral peak prominence and B, vocal efficiency for each implant and airflow rate averaged across all larynges. Implant 0 = baseline, 1 = 1386 kPa, 2 = 21.6 kPa, 3 = 9.3 kPa, 4 = 5.5 kPa. Generally, CPP and vocal efficiency decreased with increasing airflow

high-speed camera placed perpendicular to the glottal midline as described previously.[20] The two views were then used to calculate the three-dimensional (3D) medial surface contour, as described previously using an image-processing program (DaVis 8.3.1, LaVision Inc, Ypsilanti, Michigan).[20] This mapping process was calibrated using a calibration plate (25x25mm calibration target, LaVision Inc). 3D deformation calculations (medial surface displacement and contour) were performed at baseline (no implant) and for each of the four implants. Calculations were exported to MATLAB to generate 3D contour plots. Coronal sections were taken from these contour plots at the midline as well as at midway points between anterior and posterior limits of the vocal fold. Displaced medial VF surface area was calculated using ImageJ software.[21]

Kruskal-Wallis rank sum analysis, correlation coefficient analyses and linear regression analyses were performed with R software (version 3.5, R Foundation for Statistical Computing, Vienna, Austria) using Rstudio graphical user interface (version 1.1.463, Rstudio Inc, Boston, Massachusetts). Due to the small sample size in this study, all *P*-values should be considered descriptive and *P*-values <0.1 may suggest areas for further investigation. Exploratory regression analysis initially included all covariates measured but covariates with coefficients that were not significant were removed to create the most parsimonious model.

3 | RESULTS

3.1 | Effects on pressure-flow relationship

The effect of each implant on the pressure-flow relationship is shown for L2 in Figure 4. All three larynges had similar relationships between implants with some minor variability. MT implants increased the subglottal pressure achieved at a given airflow. In general, higher subglottal pressure was reached at lower airflow rates with stiffer implants. The highest airflow requirement was at baseline (no implant) while the stiffest implant (I1) required the least airflow. Softer implants required intermediate airflow. Glottal resistance (R_g) achieved with each implant was calculated as the ratio of the pressure-flow curve for each implant in each larynx (Figure 5A). In general, stiffer implants generated a larger R_g (L2 R_g by implant, I1 > 2 > 4 > 3; L1 I2 > 1 > 3 > 4; and L3 I1 > 3 > 2 > 4).

3.2 | Effects on acoustics and vocal efficiency

CPP, vocal efficiency, and F_0 were calculated at airflow rates of 200, 400, and 600 mL/s. At airflow of 200 mL/s, CPP increased with decreasing implant stiffness. As airflow increased (400 mL/s), CPP increased for the stiffer implants and became similar for all implants. However, with further increasing airflow rate (600 mL/s) CPP decreased for the softer implants and the relationship seen at the lower airflow rate reversed at the highest airflow rate. (Figure 6).

Vocal efficiency was calculated as the ratio between radiated sound power and the product of mean subglottal pressure and mean airflow rate. Across conditions, baseline and implants demonstrated decreasing vocal efficiency with increasing airflow (I2 was an outlier at 400 mL/s). Across flow rates, implants improved vocal efficiency compared to baseline, but each implant demonstrated its own unique pattern (Figure 6).

Phonation onset pressure (PTP) decreased with implant stiffness (Figure 5B). F_0 followed a similar trend, decreasing as implants became softer (data not shown).

3.3 | Effects on medial surface displacement and glottal contour

Total medial surface area displaced (D_t) was calculated in 2D (x-y) for each experimental condition. When examining the effects of implant stiffness on D_t, softer implants generally resulted in lower D_t values (Figures 3B,C and 5C). This pattern was seen in all conditions except for L3 where I2 resulted in the largest displacement (2 > 1 > 3 > 4). When comparing the maximal medial displacement (D_{max}), the stiffest implants (I1) consistently resulted in the highest D_{max} (Figure 5D). However, I2-4 showed no consistent differential pattern in D_{max} between larynges.

Coronal slices of the medial surface of the vocal fold contour were generated for each larynx and condition. Implants led to VF medialization and increased the vertical thickness of the medial surface compared to baseline (Figure 3D). The medial vocal fold contour appeared similar between implants (Figure 3D).

When correlating D_{max} and D_t with acoustic measures averaged across all airflow rates, both displacement measures had a positive correlation to F_0 (D_{max}: P = <.001, R^2 = 0.87; D_t: P = .002, R^2 = 0.56) and negative correlation to CPP (D_{max}: P = .04, R^2 = 0.29; D_t: P = .03, R^2 = 0.35). Both variables had a strong correlation with CPP at airflow of 200 (D_{max}: P = .01, R^2 = 0.44; D_t: P = .007, R^2 = 0.48) and 400 mL/s (D_{max}: P = .005, R^2 = 0.48; D_t: P = .05, R^2 = 0.48) but a weak relationship at 600 mL/s (D_{max}: P = .3, R^2 = 0.02; D_t: P = .24, R^2 = 0.06). There was no correlation between either displacement measure and PTP or mean HNR (P > .05).

4 | DISCUSSION

While MT is a common surgical treatment for glottic insufficiency, the results are quite variable. Yet, we currently lack a physiologic explanation for the variable outcomes. Although, one of the goals of MT is to improve glottal closure, glottal channel shape and vocal fold body stiffness are also concurrently changed. The roles of implant stiffness, glottal channel shape, and airflow rate on acoustic outcomes are unknown. Thus, we sought to investigate the effects of implant stiffness on the glottal channel shape and acoustics/aerodynamics. Implants of various stiffness levels that achieved complete glottal closure were used in an ex vivo human laryngeal phonation model to evaluate the effects on glottal channel shape and acoustics.

Important differences between stiff and soft implants were found in this study. Stiffer implants required higher PTP and provided increased R_g.[7] Stiffer implants displaced more medial surface area. The effects of implant stiffness on acoustics varied with airflow. Softer implants required lower PTP but required higher airflow for phonation. Softer implants improved CPP at lower airflow (200 mL/s, Figure 4), while this relationship reversed at the highest airflow (600 mL/s). Since human phonation is flow-limited (ie, lungs have a finite vital capacity), implant stiffness choice would have to consider the balance between better acoustics vs better airflow control.

While the softest implants resulted in higher CPP (better acoustic quality) at lower airflow, they became most unstable at higher airflow. As airflow increased, CPP deteriorated more for softer implants. Meanwhile, stiffer implants appear to be less optimal for lower airflow states compared to higher airflow states. These observations might explain the variable results seen with MT. Each implant stiffness, shape, and position may be beneficial for some airflow/subglottic pressure combinations but not for others. This reflects the inherent limitation of MT in that implants of a single stiffness are used, while during in vivo phonation the body-cover layer undergoes numerous changes in stiffness, tension, and glottal contour.[22] Clinically, MT has poorer outcomes in some conditions such as high vagal paralysis and significant presbylarynx/tissue atrophy. MT results are thus limited if there are limited compensatory mechanisms to change VF tension (vagal paralysis) or difficulty generating adequate airflow or subglottal pressure (presbylarynx). While stiffer implants are superior at increasing R_g and thus preventing excessive loss of vital capacity for phonation, they result in poorer acoustics at more physiologic airflow rates (200-400 mL/s). On the other hand, while softer implants have improved harmonics, they did not maintain acoustic stability at higher airflows and are likely suboptimal for loud phonation.

While we initially intended to find a correlation between glottal channel shape and acoustics, an obvious trend was not found. Although implants improved acoustics compared to baseline, the small differences in medialization (both D_{max} and D_t) between implants did not translate to differences in acoustics. The small differences in displacement between implants suggests a need to test a wider range of implant stiffnesses, as the range we used for soft implants might have been too narrow. Evaluation of implant effects on surface contour revealed small (<1 mm) differences on surface contour between implants (Figure 3D). All implants resulted in a similar medial surface contour, with a medialized VF, and a more rectangular glottis compared to no implant condition. These findings highlight some potential causes of the variable results experienced when focusing solely on glottal closure in the treatment of glottic insufficiency, since medialization alone does not necessarily correlate with acoustic measures. Thus, implant stiffness may play a larger role in optimizing acoustic outcomes.

The VF medial surface area in contact for phonation has an effect on phonation parameters. Using simple geometry to model the VFs, Zhang[23] showed that vertical thickness of the VF medial surface plays an important role in regulating the closure pattern of VF vibration and acoustics. In our study, though we were able to measure D_{max} and D_t, we did not have an effective means for measuring vertical thickness. The study by Zhang, however, suggests that the changes to vocal fold contour seen in Figure 3D would result in significant changes in the produced acoustics. Thus, any conclusions on the effects of vertical thickness on phonation require further study. Computational models with more realistic and complex geometry and ex vivo studies with more precise measurements of vertical thickness based upon the glottal contact and vibratory areas might be more accurate ways of evaluating the role of implants on VF vertical thickness, and acoustics.

Another limitation of our experimental design was that medial surface contour data were not gathered concurrently with

aerodynamic and acoustic data. Acoustics and aerodynamics were measured from a full larynx during vibration, while glottal contour was measured in a static hemilarynx model. The current method of marking the medial surface with makeup is superior for static 3D measurements but suboptimal for hemilaryngeal phonation makeup has a propensity to come off if it touches the any surface. However, hemilaryngeal phonation experiments using previously reported India ink marking methods could be considered.[1]

This study adds to our goals to improve the MT technique using silastic implants. This study is consistent with our previous study and significantly adds to it with an analysis of vocal fold contour, by comparing the medial surface displacement caused by each implant and by relating these physical changes of the vocal folds to acoustics.[7]Additionally, our prior study used only two larynges in its analysis and current findings should help strengthen the relevant conclusions by more than doubling the sample size. Computational models could be considered for future studies, however, such simulations are carried out under ideal conditions and do not account for interlaryngeal variation seen in clinical practice and thus may not reflect real-world results. Future investigations using an in vivo large animal model are planned using the findings of this pilot study as a foundation.

5 | CONCLUSIONS

A better understanding of the effects of implant stiffness, geometry, and medial surface shape is needed to improve acoustic outcomes in treating glottal insufficiency with MT. Our study showed differential flow-pressure relationships and acoustic outcomes with stiff vs soft implants. This paves the way towards developing a customized patient-specific MT implants.

CONFLICT OF INTEREST

The authors declare no potential conflict of interest.

ORCID

Brian H. Cameron https://orcid.org/0000-0001-7003-1484
Zhaoyan Zhang https://orcid.org/0000-0002-2379-6086

REFERENCES

1. Vahabzadeh-Hagh AM, Zhang Z, Chhetri DK. Three-dimensional posture changes of the vocal fold from paired intrinsic laryngeal muscles. *Laryngoscope*. 2017;127(3):656-664. https://doi.org/10.1002/lary.26145.
2. Chhetri DK, Neubauer J. Differential roles for the thyroarytenoid and lateral cricoarytenoid muscles in phonation. *Laryngoscope*. 2015;125(12):2772-2777. https://doi.org/10.1002/lary.25480.
3. Chhetri DK, Neubauer J, Bergeron JL, Sofer E, Peng KA, Jamal N. Effects of asymmetric superior laryngeal nerve stimulation on glottic posture, acoustics, vibration. *Laryngoscope*. 2013;123(12):3110-3116. https://doi.org/10.1002/lary.24209.
4. Johns MM III, Arviso LC, Ramadan F. Challenges and opportunities in the management of the aging voice. *Otolaryngol Head Neck Surg*. 2011;145(1):1-6. https://doi.org/10.1177/0194599811404640.
5. Isshiki N, Morita H, Okamura H, Hiramoto M. Thyroplasty as a new phonosurgical technique. *Acta Otolaryngol*. 1974;78(5–6):451-457.
6. Montgomery WW, Blaugrund SM, Varvares MA. Thyroplasty: a new approach. *Ann Otol Rhinol Laryngol*. 1993;102(8 pt. 1):571-579.
7. Zhang Z, Chhetri DK, Bergeron JL. Effects of implant stiffness, shape, and medialization depth on the acoustic outcomes of medialization laryngoplasty. *J Voice*. 2015;29(2):230-235. https://doi.org/10.1016/j.jvoice.2014.07.003.
8. Titze IR, Riede T, Mau T. Predicting achievable fundamental frequency ranges in vocalization across species. *PLoS Comput Biol*. 2016;12(6):e1004907. https://doi.org/10.1371/journal.pcbi.1004907.
9. Mau T, Muhlestein J, Callahan S, Chan RW. Modulating phonation through alteration of vocal fold medial surface contour. *Laryngoscope*. 2012;122(9):2005-2014. https://doi.org/10.1002/lary.23451.
10. Chan RW, Titze IR, Titze MR. Further studies of phonation threshold pressure in a physical model of the vocal fold mucosa. *J Acoust Soc Am*. 1997;101(6):3722-3727.
11. Mendelsohn A, Zhang Z. Phonation threshold pressure and onset frequency in a two-layer physical model of the vocal folds. *J Acoust Soc Am*. 2011;130(5):2961-2968. https://doi.org/10.1121/1.3644913.
12. Zhang Z. Restraining mechanisms in regulating glottal closure during phonation. *J Acoust Soc Am*. 2011;130(6):4010-4019. https://doi.org/10.1121/1.3658477.
13. Samlan RA, Story BH, Bunton K. Relation of perceived breathiness to laryngeal kinematics and acoustic measures based on computational modeling. *J Speech Lang Hear Res*. 2013;56(4):1209-1223. https://doi.org/10.1044/1092-4388(2012/12-0194).
14. Hirano M. Morphological structure of the vocal cord as a vibrator and its variations. *Folia Phoniatr (Basel)*. 1974;26(2):89-94.
15. Vahabzadeh-Hagh AM, Zhang Z, Chhetri DK. Hirano's cover-body model and its unique laryngeal postures revisited. *Laryngoscope*. 2018;128(6):1412-1418. https://doi.org/10.1002/lary.27000.
16. Chhetri DK, Zhang Z, Neubauer J. Measurement of Young's modulus of vocal folds by indentation. *J Voice*. 2011;25(1):1-7. https://doi.org/10.1016/j.jvoice.2009.09.005.
17. Chhetri DK, Berke GS, Lotfizadeh A, Goodyer E. Control of vocal fold cover stiffness by laryngeal muscles: a preliminary study. *Laryngoscope*. 2009;119(1):222-227. https://doi.org/10.1002/lary.20031.
18. Zhang Z, Neubauer J, Berry DA. The influence of subglottal acoustics on laboratory models of phonation. *J Acoust Soc Am*. 2006;120(3):1558-1569.
19. Shue YL. *The Voice Source in Speech Production: Data, Analysis and Models. [dissertation]*. Los Angeles: University of California Los Angeles; 2010.
20. Vahabzadeh-Hagh AM, Zhang Z, Chhetri DK. Quantitative evaluation of the in vivo vocal fold medial surface shape. *J Voice*. 2017;31(4):513.e15-513.e23. https://doi.org/10.1016/j.jvoice.2016.12.004.
21. Rueden CT, Schindelin J, Hiner MC, et al. ImageJ2: ImageJ for the next generation of scientific image data. *BMC Bioinformatics*. 2017;18(1):529. https://doi.org/10.1186/s12859-017-1934-z.
22. Chhetri DK, Park SJ. Interactions of subglottal pressure and neuromuscular activation on fundamental frequency and intensity. *Laryngoscope*. 2016;126(5):1123-1130. https://doi.org/10.1002/lary.25550.
23. Zhang Z. Cause-effect relationship between vocal fold physiology and voice production in a three-dimensional phonation model. *J Acoust Soc Am*. 2016;139(4):1493-1507. https://doi.org/10.1121/1.4944754.

How to cite this article: Cameron BH, Zhang Z, Chhetri DK. Effects of thyroplasty implant stiffness on glottal shape and voice acoustics. *Laryngoscope Investigative Otolaryngology*. 2020;5:82–89. https://doi.org/10.1002/lio2.322